rf conductivity of a two-dimensional electron system at small Landau-level filling factors

M. A. Paalanen, R. L. Willett, P. B. Littlewood, R. R. Ruel, K. W. West, L. N. Pfeiffer, and D. J. Bishop
AT&T Bell Laboratories, Murray Hill, New Jersey 07974
(Received 3 February 1992)

We have determined the dynamical conductivity $\sigma(k,\omega)$ of the two-dimensional (2D) electrons in extremely high-mobility GaAs/$Al_{1-x}Ga_xAs$ heterostructures by measuring the attenuation and velocity of surface acoustic waves. In the small-filling-factor limit we find a broad conductivity resonance indicating a pinning mode of the 2D electron system, which has condensed into an ordered phase. Surprisingly, the data suggest a relatively *small* correlation length even in these high-quality systems.

The phase diagram of a two-dimensional electron system (2DES) is unexpectedly rich at high magnetic fields, where the kinetic energy of the electrons is quenched by Landau quantization. In the low-disorder limit, electron correlations are determined by Coulomb interactions and the phase diagram consists of a series of incompressible liquidlike ground states at the odd-denominator fractional fillings of the lowest Landau level.[1] Coulomb interactions are also expected to solidify the 2DES into a Wigner crystal state in the high-field, low-filling-factor limit[2-4] where the solid phase should be energetically favorable.[5] While the fractional quantum Hall effect (FQHE) can survive moderate disorder, a random potential will induce a finite correlation length ξ in the Wigner crystal. An open question has been whether high-mobility heterostructures are sufficiently low in disorder to allow long correlation lengths.

Definitive determination of the crystallization has been difficult. Even in high-quality ($\mu > 10^6$ cm^2/V s) GaAs/$Al_{1-x}Ga_xAs$ heterostructures, residual disorder may play a crucial role in the small-filling-factor limit. The nature of the positional order in these systems may range from a glassy, almost single electron localization ($\xi n^{1/2} \approx 1$) to a perfect crystalline order with minimal pinning ($\xi n^{1/2} \gg 1$). Compounding the problem is the fact that most experimental techniques such as dc transport and optical measurements provide little discrimination with respect to the degree of disorder. Consequently, only indirect evidence for Wigner crystallization has been presented, and most of this has been subject to alternative interpretations. The dc resistance of the 2DES was found to increase exponentially toward lower temperatures around the $\frac{1}{5}$ fractional state.[5-7] In I-V curve measurements, one finds nonlinearities[7-10] and noise[8,10] due to the alleged depinning of the crystal. However, the value of the depinning field differs by a factor of 100 in the above references. There have also been rf conductivity measurements intended to probe the low-frequency shear mode of the solid.[11] The shear mode should not be present in the liquid and its observation would provide unambiguous proof for the existence of the solid phase. The interpretation of these data has, however, been controversial.[12] Recent optical studies[13] described a nonspecific, additional luminescence peak in the presumed Wigner crystal regime and as in the above referenced studies provide further rough characterization of the small-filling-factor limit, but cannot determine the degree of electron ordering.

In this Brief Report, we present surface-acoustic-wave (SAW) studies in high-mobility GaAs/$Al_{1-x}Ga_xAs$ samples and derive the dynamical conductivity $\sigma(k,\omega)$ of the 2DES from the attenuation and the velocity of the SAW. In the long-wavelength and low-filling-factor limit, our conductivity data describe a broad, nearly wave-vector-independent resonance at about 1 GHz in the expected Wigner crystal regime. In analogy to properties of charge-density-wave states in other materials, we interpret this resonance as the pinning mode of a disordered solid phase rather than the clean limit $\omega \propto k^{3/2}$ shear mode reported by others.[11] We can estimate the correlation length ξ from the sound wavelength and the pinning frequency. Surprisingly, the upper limit of the correlation length is only 2 μm or about 50 lattice constants.

In this experiment, we have used five low-density ($n \approx 6\times10^{10}$ cm^{-2}), high-mobility [$\mu \approx (2-4)\times10^6$ cm^2/V s] samples with the details of our sample geometry, sound transducers, and SAW measuring technique outlined previously.[14,15] Because of the piezoelectric coupling of the surface wave to the 2DEG, the attenuation and velocity of the SAW provide an indirect way of measuring the dynamical conductivity $\sigma_{xx}(k,\omega)$ of the electrons. In the ω-k plane, the SAW technique is limited to the $\omega = v_s k$ line, where v_s is the SAW velocity. The measurements are further limited by the geometry of the transducers to a discrete set of odd harmonics 1,3,5,... of the fundamental transducer frequency ω_0. By varying ω_0 and using higher harmonics we have managed to study the SAW response in our five samples between 18 MHz and 1.55 GHz with wavelengths between 150 and 2.0 μm. In these experiments, the samples were cooled to 80 mK in a dilution refrigerator inside a 165-kG superconducting magnet.

In Fig. 1 we have plotted the attenuation and velocity shift of the SAW vs magnetic field in sample 1 along with the simultaneously measured dc resistance ρ_{xx}(dc). The dc resistance shows well-developed minima at the $\frac{1}{5}$ and $\frac{2}{9}$ fractional states. The SAW response in Fig. 1 can be understood within a simple relaxation model in which the

sound attenuation and its velocity both change as a function of the dynamical conductivity $\sigma_{xx}(k,\omega)$ of the electrons.[16,17] In this model, both the attenuation

$$A = k\frac{K_{\text{eff}}^2}{2}\frac{\sigma_{xx}(k,\omega)/\sigma_m}{1+[\sigma_{xx}(k,\omega)/\sigma_m]^2} \tag{1a}$$

and the normalized velocity change

$$\frac{\Delta v}{v} = \frac{K_{\text{eff}}^2}{2}\frac{1}{1+[\sigma_{xx}(k,\omega)/\sigma_m]^2} \tag{1b}$$

are directly proportional to the piezoelectric coupling constant $K_{\text{eff}}^2/2 = 0.000\,32$ but are nonlinear functions of $\sigma_{xx}(k,\omega)$. The conductivity scale in Eq. (1) is set by $\sigma_m = (\epsilon_0+\epsilon_p)v_s = 3.6\times10^{-7}\ \Omega^{-1}$, where ϵ_0 and ϵ_p are the dielectric constants of vacuum and GaAs, respectively.[18] The theory lines in Fig. 1 are calculated from Eq. (1) using the dc conductivity values estimated from the formula $\sigma_{xx} = \rho_{xx}/(\rho_{xx}^2+\rho_{xy}^2)$, where the Hall resistance ρ_{xy} is substituted by its classical value B/ne. In Fig. 1, we have normalized the measured attenuation (velocity change) to range from 0 to 0.5 (from 0 to 1). All our fits were obtained by adjusting only one parameter, the geometrical factor used in calculating the sheet resistance per square (upper panel in Fig. 1). This geometrical factor turned out to be in agreement with the value obtained directly from the dc lead configuration. We find from Fig. 1 that using the dc conductivity in Eqs. (1) produces reasonably good agreement with the measured SAW signal between 100 and 130 kG. The SAW probes a larger sample area than the dc measurements and a 2% density gradient over the sample could explain the rounding of the SAW response at the sharp features near the $\frac{1}{5}$ and $\frac{2}{9}$ fillings. We conclude that within our accuracy $\sigma_{xx}(k,\omega)=\sigma_{xx}(\text{dc})$ for fields up to 130 kG. However at higher fields, for $\nu<\frac{1}{5}$, the large difference between the experiment and theory can only be explained by concluding that $\sigma_{xx}(k,\omega)\gg\sigma_{xx}(\text{dc})$.

The temperature dependence of the normalized SAW amplitude and velocity change are shown in Fig. 2 for sample 2 at 91 MHz and 160 kG. Again, we have used Eq. (1) with the measured dc conductivity to obtain the fits. The fits are good at higher temperatures, but, as in Fig. 1, they deviate from the experimental curves below about 200 mK. In addition, the attenuation data show a kink at 180 mK. The anomalous low-temperature features in Figs. 1 and 2 may indicate electron ordering below a magnetic-field-dependent transition temperature T_c. As outlined below, this SAW technique allows determination of both the real and imaginary $\sigma(\omega,k)$. Analysis of the measured complex conductivity in the small-filling-factor limit suggests a pinning mode in the electron solid centered near 1 GHz.

We can calculate $\sigma_{xx}(k,\omega)$ from both the sound attenuation and from the velocity by inverting Eqs. (1a) and (1b). However, we first check that the attenuation and velocity data are mutually consistent within this model. This test is done in Fig. 3 by plotting the temperature-dependent data from Fig. 2 in the velocity-attenuation plane. In this Cole-Cole plot Eq. (1) maps into a semicircle (thin lines). In Fig. 3, the 1015 MHz (11th-harmonic)

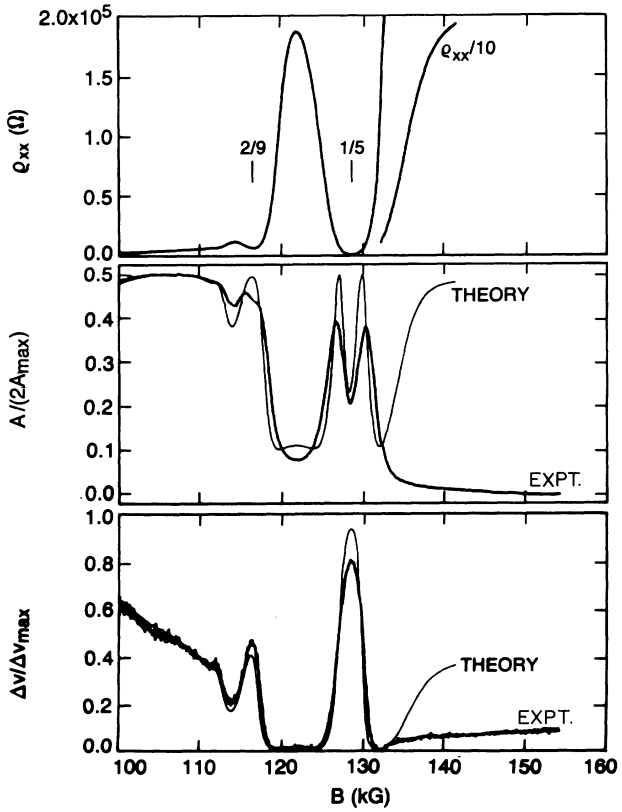

FIG. 1. Magnetic-field dependence of dc resistance ρ_{xx}, normalized SAW attenuation, and velocity shifts in sample 1 at 80 mK and 235 MHz. The theory lines are calculated from Eq. (1) using ρ_{xx}(dc).

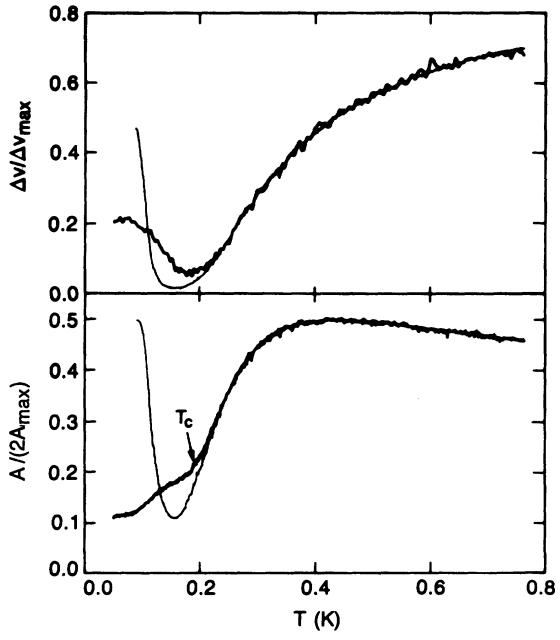

FIG. 2. Temperature dependence of normalized velocity shift and attenuation in sample 2 at 160 kG ($\nu=0.167$) and 91 MHz. The theory lines are based on Eq. (1) and on the simultaneously measured ρ_{xx}(dc) values.

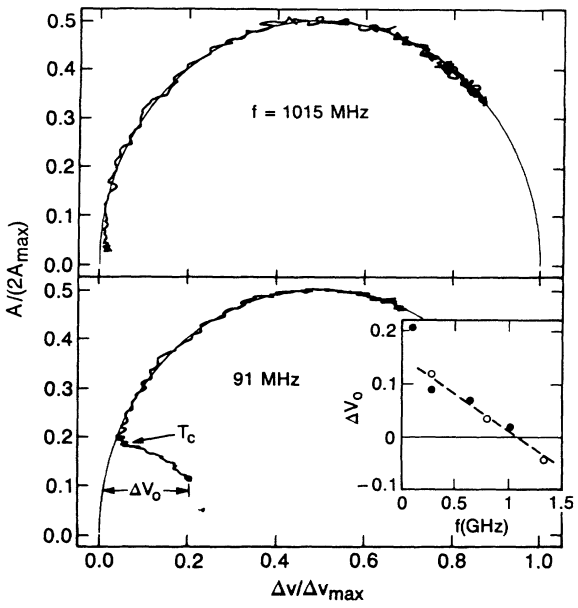

FIG. 3. A Cole-Cole type phase plot of sound attenuation vs velocity shift at two different frequencies for sample 2 at a constant B ($\nu=0.167$). The theoretical line based on Eq. (1) forms a semicircle. In the inset, Δv_0 is plotted as a function of frequency for sample 2 (○) and sample 3 (●, $\nu=0.140$).

data are in reasonable agreement with Eq. (1) but the 91-MHz data deviate sharply from the prediction of the conductivity model below the transition temperature T_c. We conclude that this breakdown of the simple conductivity model is caused by the appearance of a sizable imaginary part of the conductivity as the electrons condense into a solid phase and are pinned by disorder. In Eq. (1), the attenuation and velocity are expressed only as a function of the real part of the normalized conductivity $\sigma'=\mathrm{Re}[\sigma_{xx}(k,\omega)]/\sigma_m$. Including the imaginary part $\sigma''=\mathrm{Im}[\sigma_{xx}(k,\omega)]/\sigma_m$ in the model, we get the following, generalized equations for the normalized attenuation[16,17]

$$A/2A_{\max}=\frac{\sigma'}{(1+\sigma'')^2+(\sigma')^2} \tag{2a}$$

and for the normalized velocity shift

$$\Delta v/\Delta v_{\max}=\frac{1+\sigma''}{(1+\sigma'')^2+(\sigma')^2}\ . \tag{2b}$$

The semicircles in Fig. 3 are the $\sigma''=0$ solution of Eq. (2) in the attenuation-velocity plane and the points inside and outside the semicircle correspond, respectively, to positive and negative σ'' values. Usually, σ'' of the electron gas is small. However, in the electron solid, where there are low-frequency modes, the real and the imaginary part of the conductivity can become comparable. From the Kramers-Kronig relation we also know that σ'' should be positive below the center of the mode and change sign at the center of the mode. This is in qualitative agreement with the data shown in the inset of Fig. 3. Here Δv_0, the lowest-temperature deviation of the measured velocity from the calculated $\sigma''=0$ value, is plotted as a function of the SAW frequency. According to Eq. (2b), in the first-order approximation $\Delta v_0 \propto \sigma''$ and the linear zero crossing of the data in the inset puts the mode center at about 1 GHz.

In Fig. 4 the real part of the dynamical conductivity plotted as a function of inverse temperature also demonstrates crossing of the pinning mode. First we note that the rf conductivities approach a finite $T=0$ K value larger than $1/\rho_{xx}$(dc) (see Fig. 1). We find a sharp transition temperature T_c, below which $\sigma_{xx}(k,\omega)$ becomes frequency dependent. In sample 2, with a range of SAW frequencies from 91 to 1015 MHz $\sigma_{xx}(k,\omega)$ increased monotonically with increasing frequency at $T<T_c$ (the intermediate frequencies are not displayed). In sample 3 with higher-frequency SAW transducers we clearly see the mode crossing through a conductivity resonance. The conductivities at 270 MHz and 1.34 GHz are less than the value near the center of the mode at 807 MHz. A similar result was observed for another sample at frequencies of 300, 900, and 1500 MHz. Combining the results of Figs. 3 and 4 we conclude that at filling factors $\nu<0.170$ the 2DES has a broad pinning mode, which is centered is about 1 GHz.[19] In addition we see in the inset of Fig. 4 that the transition temperature T_c is a strong function of the filling factor ν, vanishing near the $\frac{1}{5}$ fractional state. Due to limitations on the experimentally accessible temperatures we could not determine T_c for $\nu>0.2$.

We can estimate the correlation length ξ of the electron crystal from the measured pinning frequency. In the long-wavelength $k<2\pi/\xi$ regime, the pinning frequency is constant and scales like $\omega_{\mathrm{pl}}\omega_t/\omega_c$, where the plasma frequency $\omega_{\mathrm{pl}}^2=ne^2k/2\epsilon_p m^*$ and the shear mode fre-

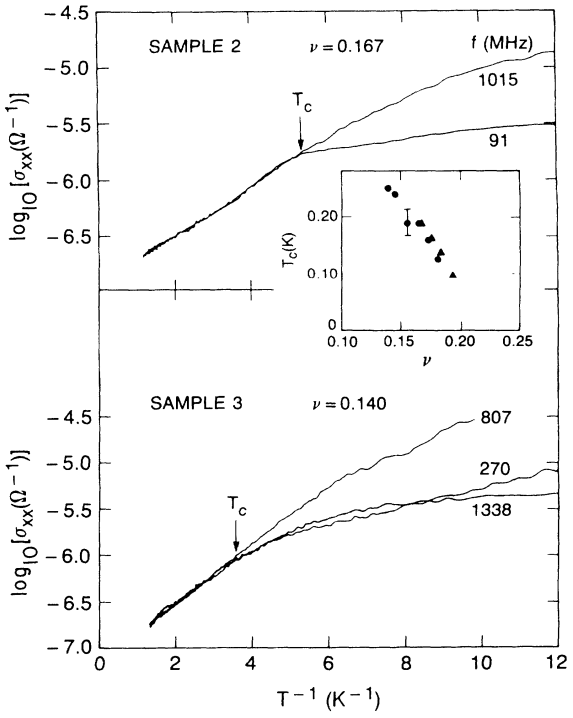

FIG. 4. High-frequency conductivity $\sigma_{xx}(k,\omega)$ of a 2DEG in the Wigner crystallization regime as a function of inverse temperature. The inset shows T_c as a function of filling factor ν.

quency $\omega_t^2=\eta k^2/nm^*$ are determined at the wave vector $k=2\pi/\xi$ and the cyclotron frequency $\omega_c=eB/m^*$. By estimating the shear modulus[20] $\eta\approx 4k_B T_c n$ from the transition temperature $T_c=200$ mK we obtain $\xi\approx 1$ μm from our measured pinning frequency at $\nu=0.167$. This value of ξ is about 25 lattice spacings of the electron crystal but still smaller than our minimum wavelength $\lambda_{\min}=2.0$ μm. Our estimate of ξ is shorter than the coherence length of 10 μm calculated within the weak pinning model from the depinning threshold electric field[8] but larger than the 0.5-μm value in Ref. 9. Because the samples used in these experiments seem to be comparable in quality, the difference presumably comes from different models used in estimating the correlation lengths. In our case, the shortest wavelength data at $\lambda_{\min}=2.0$ μm clearly rule out the possibility of a 10-μm correlation length at GHz frequencies in our samples.

Despite the fact that our data are taken at different wavelengths, one can try to test a modified f-sum rule $\int_0^\infty \sigma(\omega)d\omega=(\omega_{\rm pin}/\omega_c)\pi ne^2/2m^*$ for the pinning mode.[21] By assuming a Lorentzian line shape for the zero-temperature pinning mode at $\omega_{\rm pin}\approx 1$ GHz, a width of the order of 0.3 GHz and a peak conductivity value of $\approx 3\times 10^{-5}$ Ω^{-1} from Fig. 4, we find that the sum rule is satisfied to within a factor of 2. This is consistent with the k independence of the pinning mode in our low-frequency regime.

In the low-frequency hydrodynamical regime $\omega<\omega_\xi(T)=\sigma_{xx}({\rm dc})/\epsilon_p\xi$, the damping of the pinning mode is expected to be due to dc shielding currents and proportional to $\sigma_{xx}({\rm dc})$.[22] As seen in other charged-density-wave systems and discussed in Ref. 22, this damping will increase the low-frequency spectral weight of the pinning mode and is in qualitative agreement with the larger than expected $\Delta\nu_0$ at the $\omega\rightarrow 0$ limit in the inset of Fig. 3. This is also in qualitative agreement with our data in Fig. 4 where the low-temperature sharpening of the pinning mode is accompanied by a decrease of $\sigma_{xx}({\rm dc})\approx 1/\rho_{xx}({\rm dc})$. In addition, $\omega_\xi(T)\rightarrow 0$ in the low-temperature limit, and part of the frequency-dependent conductivity in Fig. 4 could be due to the low-temperature crossover from a hydrodynamical to a collisionless regime.

In conclusion, we have demonstrated a broad conductivity resonance in a 2DES in the low-temperature, high-magnetic-field limit. We interpret this as a pinning mode of the Wigner crystal with a small correlation length.

We would like to thank Andy Millis and Bruce Normand for useful discussions during this work.

[1]D. C. Tsui, H. L. Stormer, and A. C. Gossard, Phys. Rev. Lett. **48**, 1559 (1982).

[2]Y. E. Lozovik and V. I. Yudson, Pis'ma Zh. Eksp. Teor. Fiz. **22**, 26 (1975) [JETP Lett. **22**, 11 (1975)].

[3]P. K. Lam and S. M. Girvin, Phys. Rev. B **30**, 473 (1984).

[4]D. Lesvesque, J. J. Weis, and A. M. McDonald, Phys. Rev. B **30**, 1056 (1984).

[5]H. W. Jiang, R. L. Willett, H. L. Stormer, D. C. Tsui, L. N. Pfeiffer, and K. W. West, Phys. Rev. Lett. **65**, 633 (1990).

[6]R. L. Willett, H. L. Stormer, D. C. Tsui, L. N. Pfeiffer, K. W. West, and K. W. Baldwin, Phys. Rev. B **38**, 7881 (1989).

[7]R. L. Willett, H. L. Stormer, D. C. Tsui, L. N. Pfeiffer, K. W. West, M. Shayegan, M. Santos, and T. Sajoto, Phys. Rev. B **40**, 6432 (1989).

[8]V. J. Goldman, M. Santos, M. Shayegan, and J. E. Cunningham, Phys. Rev. Lett. **65**, 2189 (1990).

[9]F. I. B. Williams, P. A. Wright, R. G. Clark, E. Y. Andrei, G. Deville, D. C. Glattli, O. Probst, B. Etienne, C. Dorin, C. T. Foxon, and J. J. Harris, Phys. Rev. Lett. **66**, 3285 (1991).

[10]Y. P. Li, T. Sajato, L. W. Engel, D. C. Tsui, and M. Shayegan (unpublished).

[11]E. Y. Andrei, G. Deville, D. C. Glattli, F. I. B. Williams, E. Paris, and B. Etienne, Phys. Rev. Lett. **60**, 2767 (1988).

[12]H. L. Stormer and R. L. Willett, Phys. Rev. Lett. **62**, 972 (1989).

[13]H. Buhmann, W. Joss, K. v. Klitzing, I. V. Kukushkin, G. Martinez, A. S. Plaut, K. Ploog, and V. B. Timofeev, Pis'ma Zh. Eksp. Teor. Fiz. **52**, 925 (1990) [JETP Lett. **52**, 306 (1990)].

[14]R. L. Willett, M. A. Paalanen, R. R. Ruel, K. W. West, L. N. Pfeiffer, and D. J. Bishop, Phys. Rev. Lett. **65**, 112 (1990).

[15]A. Wixforth, J. P. Kotthaus, and G. Weimann, Phys. Rev. Lett. **56**, 2104 (1986).

[16]A. R. Hutson and D. L. White, J. Appl. Phys. **33**, 40 (1962).

[17]K. A. Ingebrigtsen, J. Appl. Phys. **41**, 454 (1970).

[18]The electron diffusivity D can be included in Eq. (1) by replacing σ_{xx} with $\sigma_{xx_{\rm eff}}=\sigma_{xx}/(1-jDk^2/\omega)$. Because $D\approx l_B^2/\tau\ll v_s^2/\omega$, the effect is small. In the above estimate $\tau\approx\hbar/\Delta E$, where $\Delta E\approx 1$ K is the width of the Landau level for our high-mobility electron gas. Equation (1) is also valid only when the wavelength $\lambda>l_{\rm in}$, where $l_{\rm in}$ is an intrinsic length scale of the systemlike mean free path of the current carriers. In high magnetic field the relevant length scale is l_B, which is less than 100 Å and our wavelength λ. For the D and $l_{\rm in}$ estimates see T. Ando *et al.*, Rev. Mod. Phys. **54**, 437 (1982), p. 539. Also σ_m is slightly frequency dependent and can be calculated from

$$\sigma_m=\sigma_m(0)\epsilon_p e^{kd}/[\epsilon_p\cosh(kd)+\epsilon_0\sinh(kd)]\ ,$$

where d is the distance between the free surface and the 2DES. See, for example, A. L. Efros and Yu. M. Galperin, Phys. Rev. Lett. **64**, 1959 (1990).

[19]Wassermeyer *et al.* [Phys. Rev. B **41**, 10287 (1990)] found recently edge magnetoplasmons (EMP) in the 2DES in GaAs. Based on their results, in our samples (3×5 mm^2) the EMP resonance should be below 50-MHz frequencies for $\nu=0.2$. We also estimate the coupling between the SAW and EMP to be extremely weak.

[20]J. M. Kosterlitz and D. J. Thouless, J. Phys. C **6**, 1181 (1973); D. R. Nelson and B. I. Halperin, Phys. Rev. B **19**, 2457 (1979).

[21]H. Fukuyama, and P. A. Lee, Phys. Rev. B **18**, 6245 (1978); most of the spectral weight for the sum rule is under the cyclotron resonance peak at ω_c.

[22]P. B. Littlewood, Phys. Rev. B **36**, 3108 (1987); B. G. Normand, A. J. Millis, and P. B. Littlewood (unpublished).